Cell, Vol. 123, 133–144, October 7, 2005, Copyright ©2005 by Elsevier Inc. DOI 10.1016/j.cell.2005.08.037

GPCR Signaling Is Required for Blood-Brain Barrier Formation in *Drosophila*

Tina Schwabe,[1] Roland J. Bainton,[3,4] Richard D. Fetter,[2] Ulrike Heberlein,[3] and Ulrike Gaul[1,*]

[1]Laboratory of Developmental Neurogenetics
[2]Laboratory of Neural Circuits and Behavior
Rockefeller University
New York, New York 10021
[3]Department of Anatomy
University of California, San Francisco
San Francisco, California 94143

Summary

The blood-brain barrier of *Drosophila* is established by surface glia, which ensheath the nerve cord and insulate it against the potassium-rich hemolymph by forming intercellular septate junctions. The mechanisms underlying the formation of this barrier remain obscure. Here, we show that the G protein-coupled receptor (GPCR) Moody, the G protein subunits Gαi and Gαo, and the regulator of G protein signaling Loco are required in the surface glia to achieve effective insulation. Our data suggest that the four proteins act in a complex common pathway. At the cellular level, the components function by regulating the cortical actin and thereby stabilizing the extended morphology of the surface glia, which in turn is necessary for the formation of septate junctions of sufficient length to achieve proper sealing of the nerve cord. Our study demonstrates the importance of morphogenetic regulation in blood-brain barrier development and places GPCR signaling at its core.

Introduction

The complex nervous systems of higher animals are insulated from the body fluid by an impenetrable blood-brain barrier. In *Drosophila*, as in other insects, this barrier serves primarily as a shield against the high potassium levels of the hemolymph: if the barrier is compromised, action potentials can no longer propagate, and the animal is paralyzed. The barrier is established at the end of embryonic development by a thin layer of epithelial cells, which are thought to be glia derived from the neural ectoderm, named surface glia. This glial epithelium ensheathes the entire nerve cord and generates an ionic seal by forming intercellular septate junctions (SJs) (Carlson et al., 2000; Edwards et al., 1993). A similar process occurs in the PNS, where peripheral glia form a single-cell tube that envelops the nerve and is sealed by autic SJs (Auld et al., 1995; Baumgartner et al., 1996).

The cellular and molecular processes involved in the ensheathment of the nervous system are generally not well understood. In the CNS, the study of the blood-brain barrier has been hampered by technical difficulties. The surface glia are extremely thin and delicate and complete their seal only at the very end of embryogenesis, making their visualization and phenotypic analysis challenging. In the PNS, Rho family GTPases and a PAK-like serine-threonine kinase (Fray) have been shown to be required for establishing or maintaining the glial ensheathment of peripheral nerves (Leiserson et al., 2000; Sepp and Auld, 2003).

By contrast, SJ formation has been studied extensively, but mostly in columnar epithelia such as the ectoderm and the trachea (for review, see Tepass et al., 2001). SJs contain regularly spaced, electron-dense septa that give them a ladder-like appearance. The septa are thought to serve as a series of filters that impede the penetration of small molecules through the intercellular cleft; the more septa are arrayed, the tighter the seal (Abbott, 1991). The SJ consists of a large complex of transmembrane and intracellular proteins, including Neurexin IV, Neuroglian, Contactin, Coracle, and the sodium pump. It is not clear to what extent the glial SJ mirrors the ectodermal SJ; to date, two of the molecular components of the ectodermal SJ have been shown to be functional in peripheral glia. The fly SJ shows striking structural, molecular, and functional similarity to the vertebrate paranodal junction, which is formed between neurons and myelinating glial cells (Poliak and Peles, 2003; Salzer, 2002).

G protein-coupled receptors (GPCRs) are a large and diverse superfamily of receptors that share a seven-transmembrane-domain structure and interact with a wide range of extracellular ligands. They transduce their signal mostly through trimeric G proteins, which consist of three subunits (α, β, and γ). Upon ligand binding, the GPCR catalyzes the exchange of GDP for GTP at Gα, leading to dissociation of the complex into Gα and Gβγ. Once separated, Gα-GTP and Gβγ can each interact with downstream effectors. Signaling is terminated by GTP hydrolysis, which is stimulated by RGS (*r*egulator of *G* protein *s*ignaling) molecules; reassociation of Gα-GDP with Gβγ completes the cycle (Neer, 1995). Our understanding of the role of GPCRs and trimeric G proteins in metazoan development is limited to relatively few examples, including germ-cell migration; asymmetric cell division; and, most recently, Wnt and planar polarity signaling (Katanaev et al., 2005; Knoblich, 2001; Kunwar et al., 2003; Schier, 2003). A role for G protein signaling in *Drosophila* blood-brain barrier formation was first suggested by the identification of the RGS *loco*, which is expressed in the surface glia and shows locomotion defects as a mutant (Granderath et al., 1999). However, Loco's cellular function has not been elucidated, nor has it been placed in a genetic pathway.

In a reverse genetic screen for factors with glial expression and function, we identified two GPCRs of a small novel Rhodopsin family, *moody* and *tre1*, as well as *loco*. Here we show that *moody*, *loco*, and the Gα genes *Gi* and *Go* are (differentially) expressed in the

*Correspondence: gaul@mail.rockefeller.edu
[4]Present address: Department of Anesthesia, University of California, San Francisco, San Francisco, California 94143.

surface glia; Moody and Loco colocalize at the plasma membrane, and Loco physically interacts with both Gi and Go, suggesting that the four proteins are part of a common signaling pathway. Using dye penetration into the nerve cord as an assay, we show that all four factors are required for proper insulation of the nervous system. Interestingly, loss and gain of signal cause qualitatively similar insulation defects, strongly suggesting that the signal is graded or localized within the cell. Using live imaging and transmission electron microscopy, we examine the cellular function of the signaling components in the morphogenesis of the surface glia and in the establishment of the intercellular SJs that generate the seal.

Results

The Development of the Surface Glial Sheath

The *Drosophila* nerve cord is ensheathed by a thin single-layer epithelium, which in turn is surrounded by an acellular layer of extracellular matrix material. Ultrastructural analysis had revealed that SJs between the epithelial cells are responsible for the insulation of the nerve cord (Carlson et al., 2000; Edwards et al., 1993). Independent fate-mapping studies showed that the nerve cord is enveloped by glia expressing the glial-specific marker Repo (Halter et al., 1995; Ito et al., 1995; Schmidt et al., 1997), but to date there has been no direct proof that it is these surface glia that form intercellular SJs and thus the insulating sheath. Moreover, the time course for the formation of the sheath and of the SJ-mediated seal has not been established.

We developed several assays to follow the morphogenesis of the surface glial sheath. Due to the onset of cuticle formation, immunohistochemistry becomes unreliable after 16 hr of development. We therefore used live imaging of GFP-tagged marker proteins to visualize cell shapes, in particular the actin cytoskeleton marker GFP/RFP-Moesin (Edwards et al., 1997) and the SJ marker Neuroglian (Nrg)-GFP (Morin et al., 2001). We find that Nrg-GFP expressed under its own promoter and RFP-Moesin driven by *repo-Gal4* are colocalized in the same cells, establishing that the SJ-forming cells are *repo* positive (Figure 1N) and thus conclusively demonstrating the insulating function of the surface glia. To probe the permeability of the transcellular barrier, we injected fluorescent dye into the body cavity and quantified dye penetration into the nerve cord by determining mean pixel intensity in sample sections (see Experimental Procedures).

The surface glia are born in the ventrolateral neuroectoderm and migrate to the surface of the developing nerve cord (Ito et al., 1995; Schmidt et al., 1997), where they spread until they touch their neighbors (17 hr of development). The glia then join to form a contiguous sheet of square or trapezoidal cells, tiled to form three-cell corners (Figures 1A–1C). SJ material is visible as a thin contiguous belt by 18 hr but continues to accumulate until the end of embryogenesis (Figures 1D–1F). Similar to other secondary epithelia, the surface glia do not form a contiguous adherens-junction belt (zonula adherens), but only spotted adherens junctions, as visualized by Armadillo-GFP (driven by own promoter; McCartney et al., 2001; Figure 1M). At 16 hr, the fluorescent dye freely penetrates into the nerve cord, but by 20 hr the nerve cord is completely sealed (Figures 1G–1I). The completion of the seal thus coincides with the onset of visible movements in the late embryo.

To further gauge our dye-penetration assay, we examined embryos mutant for known septate-junction components: Neurexin IV, which is required for blood-nerve barrier formation in the PNS (Baumgartner et al., 1996); Neuroglian; and the sodium-pump component Nervana2, for which only a role in the earlier formation of the ectodermal seal has been demonstrated (Genova and Fehon, 2003). In all three mutants, we found severe penetration of dye well after the nerve cord is sealed in wild-type (22 hr, Figures 1J–1L). These findings provide further evidence that the sealing of the nerve cord is achieved by SJs and suggest that the components of the ectodermal SJs are required for the function of surface glial SJs as well.

Moody is Expressed in Surface Glia Together with Known G Protein Signaling Components

In a genome-wide screen for glial genes, using FAC sorting of GFP-labeled embryonic glia and Affymetrix microarray expression analysis (H. Courvoisier, D. Leaman, J. Fak, N. Rajewsky, and U.G., unpublished data), we identified two novel GPCRs, Moody (CG4322; Bainton et al., 2005 [this issue of *Cell*]; Freeman et al., 2003; Kunwar et al., 2003) and Tre1 (CG3171; Kunwar et al., 2003). Both are orphan receptors belonging to the same novel subclass of Rhodopsin-family GPCRs (Kunwar et al., 2003). We examined their expression by RNA in situ hybridization; different subtypes of glia in the embryonic nerve cord can be distinguished based on their position and morphology (Ito et al., 1995). In the CNS, *moody* is expressed in surface glia from embryonic stage 13 onward (10 hr); in addition to cells surrounding the nerve cord (subperineurial glia), this includes cells lining the dorsoventral channels (channel glia). *moody* is also expressed in the ensheathing glia of the PNS (exit and peripheral glia) (Figure 2A). Both CNS and PNS expression of *moody* are lost in mutants for the master regulator of glial fate, *glial cells missing* (gcm^{N17}; Jones et al., 1995), confirming that they are indeed glial (Figure 2B). *tre1* is expressed in all longitudinal glia and a subset of surface glia, as well as in cells along the midline. As expected, the (lateral) glial expression is lost in *gcm* mutants, while midline expression is not (Figures 2C and 2D). Both *moody* and *tre1* are also expressed outside the nervous system in a largely mutually exclusive manner, specifically in the germ cells, the gut, and the heart.

Several additional G protein signaling components are found in the surface glia. The six extant Gα genes show broad and overlapping expression in embryogenesis, with three of them (*Go*, *Gq*, and *Gs*) expressed throughout the nervous system and *Gi* expressed more specifically in surface glia (Figures 2G and 2H; Parks and Wieschaus, 1991; Quan et al., 1993; Wolfgang et al., 1990); *Gβ13F* and *Gγ1* are ubiquitously expressed during embryogenesis (Schaefer et al., 2001; Yarfitz et al., 1988). Finally, the RGS *loco* is uniformly expressed in early embryos due to a maternal contribution but is

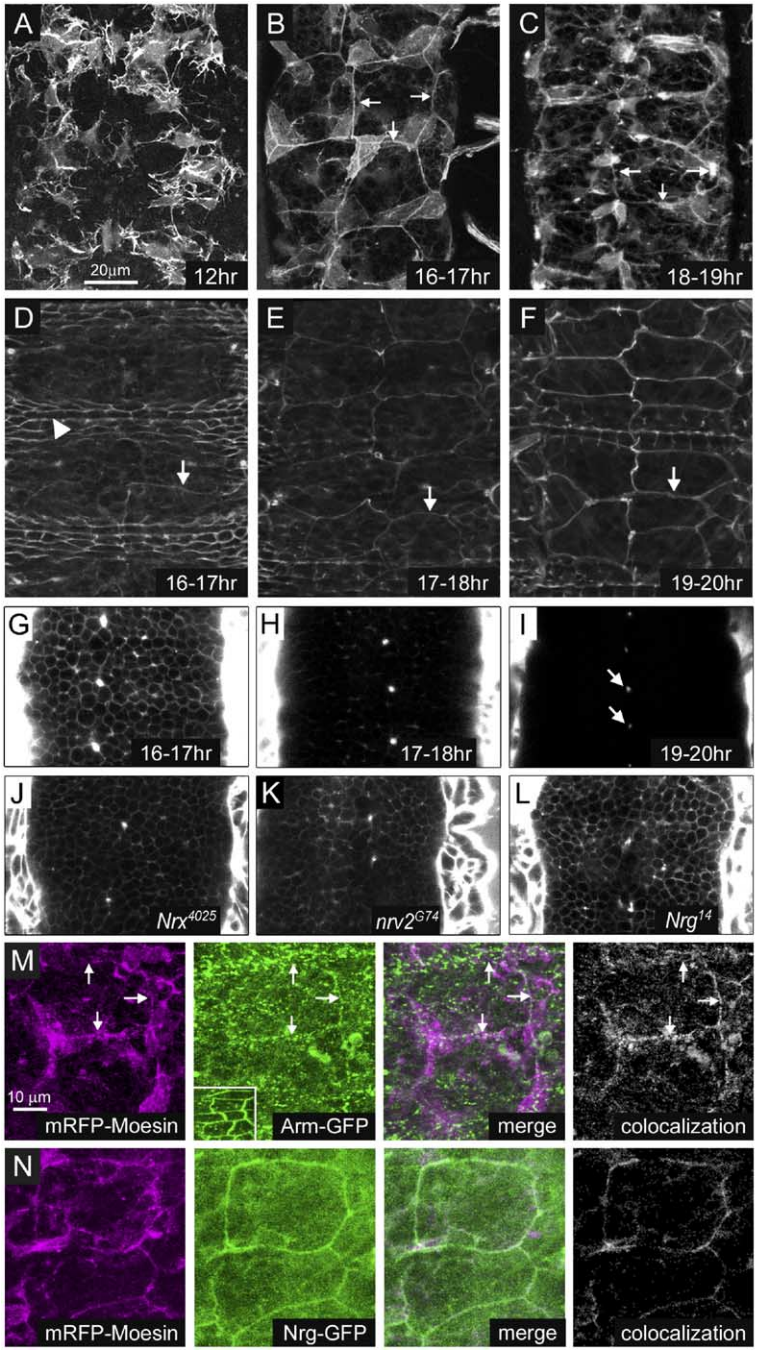

Figure 1. Developmental Time Course of the Morphogenesis and Sealing of the Surface Glial Epithelium

Images represent projections from stacks of confocal sections, 10–15 μm total (A–F, M, and N), or single confocal sections (G–L). Colocalization (M and N) was calculated in individual confocal sections and projected as described in Experimental Procedures.

(A–C) Ventral surface views of nerve cords expressing the live actin marker GFP-Moesin driven by panglial *repo-Gal4*. The epithelium becomes confluent and shows strong accumulation of cortical actin at ~16 hr (arrows); cell-shape changes from square to rectangular occur during condensation of the nerve cord (16–24 hr).

(D–I) Ventral surface views (D–F) of nerve cords expressing the live SJ marker Nrg-GFP (expressed under own promoter), which also labels the overlying ectoderm (arrowhead). With increasing accumulation of SJ material in a circumferential belt (arrows), penetration of dye from the body cavity into the nerve cord decreases (G–I); by 20 hr, the nerve cord is completely sealed. Arrows in (I) point to the location of the channels that traverse the nerve cord along its dorsoventral axis.

(J–L) In mutants of SJ components, such as Neurexin IV (Nrx^{4025}), Nervana2 ($nrv2^{G74}$), and Neuroglian (Nrg^{14}), the dye still penetrates into the nerve cord at 22 hr.

(M) Adherens junctions visualized by Arm-GFP (expressed under own promoter); for reference, the actin cytoskeleton is labeled with mRFP-Moesin (driven by *repo-Gal4*). In the surface glia, Arm-GFP shows a spotted distribution along the cell perimeter (arrows) and within the cell; by contrast, in the ectoderm (inset), the distribution along the perimeter is contiguous.

(N) SJs (visualized by Nrg-GFP, green) are formed by surface glia, as shown by colocalization with mRFP-Moesin driven by *repo-Gal4* (magenta).

then transcriptionally upregulated in surface and longitudinal glia, as well as in other tissues outside the nervous system. The nervous-system expression of *loco* is lost in *gcm* mutants (Figures 2E and 2F; Granderath et al., 1999). The presence of both Moody and Loco protein in the surface glia is confirmed using immunohistochemistry (Figures 2I and 2J), but at 17 hr of development, when staining is feasible, the protein levels are still quite low.

In sum, the GPCR Moody, the RGS Loco, and *Gi* are differentially expressed in surface glia. This expression precedes and accompanies the morphogenesis and sealing of the surface glial sheath.

Colocalization and Physical Interaction of GPCR Signaling Components

To examine protein expression and distribution of the GPCR signaling components in greater detail, we turned to third-instar larval nerve cords. By this stage, the surface glia have doubled in size and show robust protein expression of GPCR signaling and SJ components.

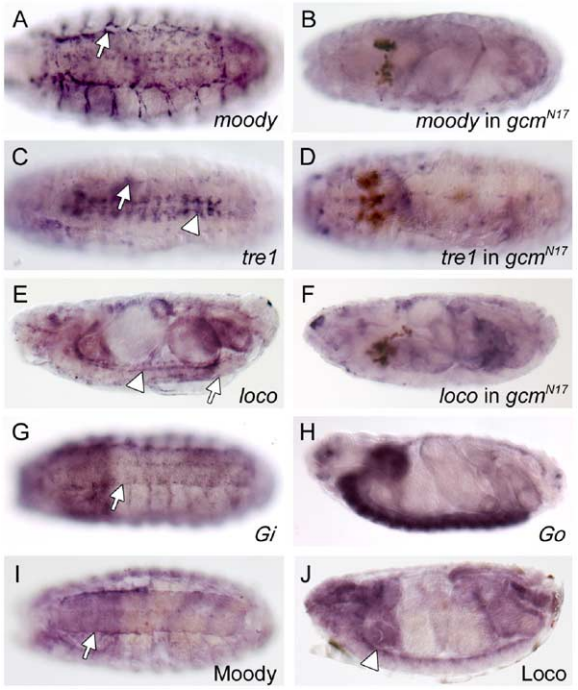

Figure 2. The GPCRs *moody* and *tre1*, the Gα Genes *Gi* and *Go*, and the RGS *loco* Are Expressed in Surface and Other CNS Glia

Expression is visualized by RNA in situ hybridization (A–H) or immunohistochemistry (I and J) at 17 hr development; lateral (E, F, H, and J) or ventral (A–D, G, and I) views. Arrows mark surface glia; arrowheads mark longitudinal glia.

(A, B, and I) *moody* RNA (A) and protein (I) are expressed in surface glia, as well as in PNS glia and in the gut; in *gcm* mutants (B), in which all glia are lost, only gut expression remains.

(C and D) *tre1* RNA is expressed in longitudinal glia, a small subset of surface glia, and in midline cells (C); in *gcm* mutants (D), glial but not midline expression is lost.

(E, F, and J) *loco* RNA (E) and protein (J) are expressed in surface and longitudinal glia, as well as in the gut and heart; in *gcm* mutants (F), only gut and heart expression remains.

(G) *Gi* RNA is differentially expressed in surface glia.

(H) *Go* is expressed ubiquitously throughout the CNS.

Moody immunostaining is found at the plasma membrane, where it shows strong colocalization with the SJ marker Nrg-GFP (Figure 3C). Loco immunostaining is punctate and more disperse throughout the cytoplasm, with some accumulation at the plasma membrane, where it colocalizes with Moody (Figure 3A). To avoid fixation and staining artifacts, we generated fluorescent-protein fusions (Moody-mRFP; Loco-GFP) and expressed them using *moody-Gal4*, which drives weak surface glial expression (see Figure S1 in the Supplemental Data available with this article online). In the live nerve-cord preparations, Loco-GFP is much less disperse and shows strong colocalization with Moody-mRFP at the plasma membrane (Figure 3B).

In the absence of a known ligand, the coupling of G proteins to receptors is difficult to establish, but their binding to RGS proteins is readily determined. Loco physically binds to and negatively regulates Gi (Granderath et al., 1999; Yu et al., 2005), and vertebrate Loco homologs (RGS12/14) have been shown to negatively regulate Gi/Go (Cho et al., 2000; Snow et al., 1998). In S2 tissue-culture assays, we find that Loco binds to Gi and Go, but not to Gs and Gq, in line with the previous results (Figure 3F). Double-label immunohistochemistry confirms that both Gi and Go are expressed in the surface glia (Figures 3D and 3E).

Thus, Loco physically interacts with Gi and Go and shows subcellular colocalization with Moody, suggesting that the four signaling components are part of a common molecular pathway.

Moody and Loco Are Required for Insulation

Using dye penetration as our principal assay, we examined whether the GPCR signaling components that are expressed in surface glia play a role in insulation. *moody* genomic (*Δ17*; Bainton et al., 2005) and RNAi mutants show similar, moderate insulation defects (Figures 4A–4C; see Experimental Procedures). The embryos are able to hatch but show mildly uncoordinated motor behavior and die during larval or pupal stages. The dye-penetration defect of $moody^{\Delta 17}$ is completely rescued by genomic rescue constructs containing only the *moody* ORF. Both *moody* splice forms (α and β; Bainton et al., 2005) are able to rescue the defect independently, as well as in combination (Figure 4E). *tre1* genomic (Kunwar et al., 2003) and RNAi mutants show no significant dye-penetration defect and no synergistic effects when combined with *moody* using RNAi (data not shown). Thus, despite the close sequence similarity of the two GPCRs and their partially overlapping expression in surface glia, only *moody* plays a significant role in insulation. Overexpression of *moody* causes intracellular aggregation of the protein (data not shown).

loco is expressed both maternally and zygotically. Granderath et al. (1999) had shown that *loco* zygotic nulls are paralytic and suggested, on the basis of an ultrastructural analysis, a disruption of the glial seal (see below). In our dye-penetration assay, *loco* zygotic null mutants show a strong insulation defect, which can be rescued by panglial expression of Loco in its wt or GFP-tagged form (Figures 4A, 4B, and 4E). The extant null allele of *loco* (*Δ13*) did not yield germline clones; we therefore used *loco* RNAi to degrade the maternal in addition to the zygotic transcript. In *loco* RNAi embryos, dye penetration is indeed considerably more severe (Figures 4B and 4C). Overall, insulation as well as locomotor behavior is affected much more severely in *loco* than in *moody* and is close in strength to the SJ mutants. Overexpression of *loco* is phenotypically normal (data not shown).

Thus, positive (*moody*) and negative (*loco*) regulators of G protein signaling show qualitatively similar defects in loss of function, suggesting that both loss and gain of signal are disruptive to insulation. Such a phenomenon is not uncommon and is generally observed for pathways that generate a localized or graded signal within the cell (see Discussion).

G Protein Function in Insulation

Both *Gi* and *Go* have a maternal as well as a zygotic component. *Gi* zygotic null flies survive into adulthood but show strong locomotor defects (Yu et al., 2003). In

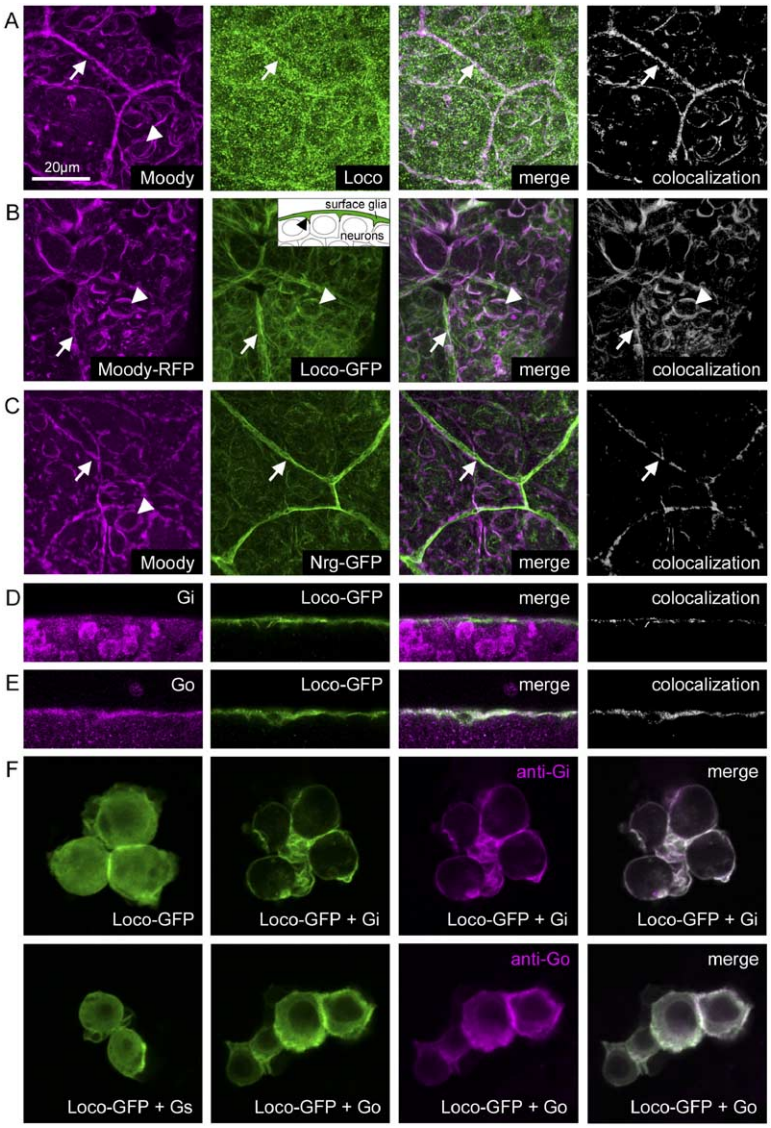

Figure 3. Colocalization and Physical Interaction of G Protein Signaling Components

(A–C) Projections of confocal stacks (5–7.5 μm) from third-instar larvae, ventral surface views.

(A) Moody (magenta) and Loco (green) antibody stainings of fixed tissue. (B) Live imaging of Moody-RFP (magenta) and Loco-GFP (green) driven by the surface-glial-specific *moody-Gal4*. Moody is found predominantly at the plasma membrane; visible are the cell boundaries between the surface glia (arrows), as well as surface glial extensions into the paracellular space between underlying neuronal cell bodies (arrowheads; inset). Loco is more broadly distributed within the cell but strongly colocalizes with Moody at the plasma membrane.

(C) Moody protein (magenta) colocalizes with the SJ marker Nrg-GFP (green).

(D and E) Gi or Go (magenta) and Loco-GFP (driven by *moody-Gal4*; green) antibody stainings of fixed larval tissue, showing coexpression in the surface glia; single confocal sections, lateral view.

(F) Transiently transfected S2 cells expressing Loco-GFP (driven by *actin-Gal4*; green) alone or together with different Gα subunits (magenta). Loco-GFP by itself localizes to cytoplasm/nucleus. In the presence of Gi or Go, but not Gs, it relocalizes to cytoplasm/plasma membrane.

our assay, *Gi* maternal and zygotic null embryos show a mild dye-penetration defect, which is markedly weaker than that of *moody* (Figures 4A and 4B), suggesting redundancy among Gα subunits. To further probe Gi function, we overexpressed the wt protein (Gi-wt) as well as a constitutively active version (Gi-GTP) (Schaefer et al., 2001) in glia using *repo-Gal4*; such overexpression presumably leads to a masking of any local differential in endogenous protein distribution. Expression of Gi-wt results in very severe dye penetration, while overexpression of Gi-GTP is phenotypically normal (Figures 4A and 4B). Only Gi-wt but not Gi-GTP can complex with Gβγ; overexpression of Gi-wt thus forces Gβγ into the inactive trimeric state. Our result therefore suggests that the phenotypically crucial signal is not primarily transduced by activated Gi but rather by free Gβγ. Similar results have been obtained in the analysis of Gi function in asymmetric cell division (Schaefer et al., 2001; Yu et al., 2003).

Go null germline clones do not form eggs and do not survive in imaginal discs, indicating an essential function for cell viability (Katanaev et al., 2005). We therefore examined animals with glial overexpression of constitutively active (Go-GTP), constitutively inactive (Go-GDP), and wt (Go-wt) Go (Katanaev et al., 2005). Overexpression of Go-GDP, which cannot signal but binds free Gβγ, leads to severe dye penetration, again pointing to a requirement for Gβγ in insulation. However, Go-GTP and Go-wt show a moderate effect, suggesting that signaling by active Go does contribute significantly to insulation, in contrast to active Gi (Figures 4A and 4B).

Overall, we find that all four GPCR signaling components expressed in surface glia are required for insulation, further supporting the notion that the four components are part of a common pathway. The phenotypic data suggest that this pathway is complex: two Gα proteins, Gi and Go, are involved, but with distinct roles: activated Go and Gβγ appear to mediate most of the signaling to downstream effectors, while activated Gi

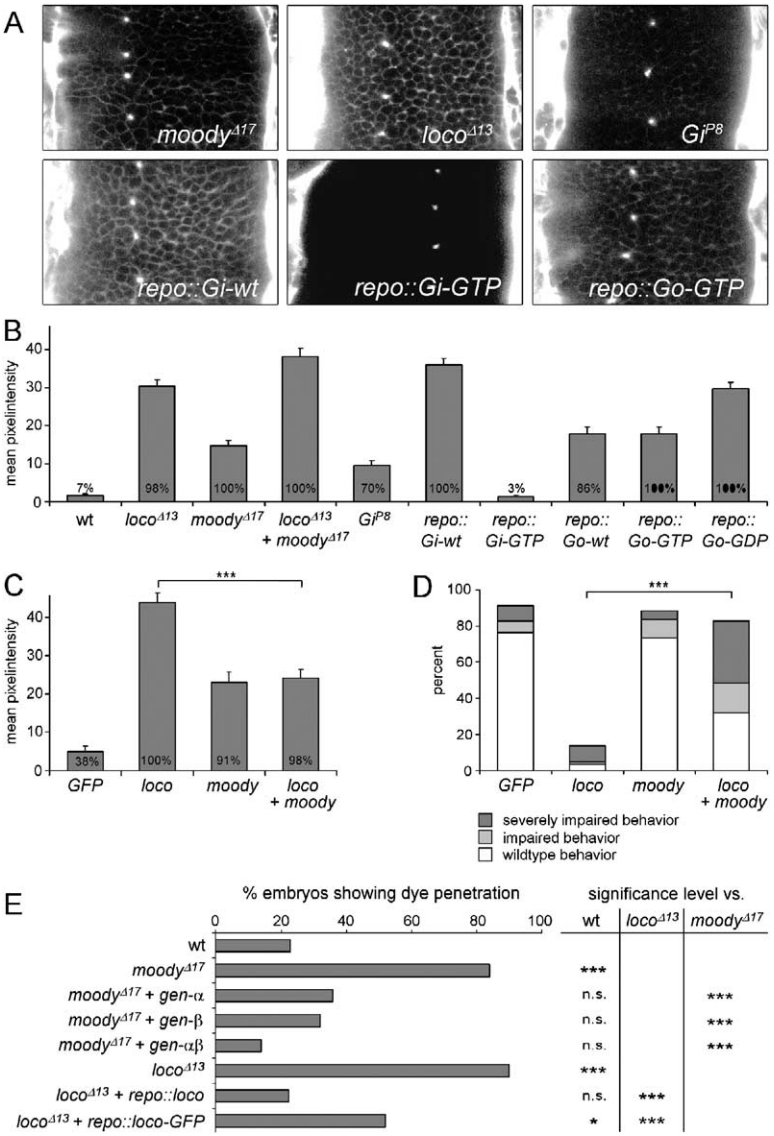

Figure 4. Normal *moody*, *loco*, and G Protein Activity Are Required for Proper Insulation of the Nerve Cord

(A) Single confocal sections of dye-injected embryos of different genotypes, showing different levels of dye penetration into the nerve cord.

(B and C) Quantification of results of dye-penetration assays. Columns represent intensity of dye penetration as measured by mean pixel intensity (see Experimental Procedures), ±SEM, n = 34–55. The percentage of embryos showing dye penetration is indicated at the bottom of each column.

(B) Genomic mutants and embryos overexpressing UAS transgenes. All groups except *repo::Gi-GTP* are significantly different from wt with $p < 0.01$.

(C) RNAi-injected animals are shown separately since dye penetration increases slightly when mock or dsRNA injection is performed in addition to the late dye injection. Brackets and asterisks in (C)–(E) indicate significance levels of pairwise comparisons using one-way ANOVA with Student-Newman-Keuls post hoc test (C) or the χ^2 test (D and E): n.s. $p > 0.05$; *$p < 0.05$; ***$p < 0.001$.

(D) The locomotor behavior of RNAi-injected animals is assessed by hatching rate (total height of bars), presence or absence of peristalsis, and general motility (Experimental Procedures; see Movies S1–S3).

(E) The ability of different *moody* and *loco* transgenes to rescue their cognate genomic mutant was assessed by determining the percentage of embryos showing dye penetration (n = 40–57).

seems to function primarily as a positive regulator of Gβγ. The loss of *moody* appears much less detrimental than the loss of free Gβγ (through overexpression of Gi-wt or Go-GDP); this is inconsistent with a simple linear pathway and points to additional input upstream or divergent output downstream of the G proteins (see Discussion). Finally, we consistently observe that both loss (*moody*, *Gi* null, and Go-GDP) and gain (*loco* and Go-GTP) of signal are disruptive to insulation, suggesting that the G protein signal or signals have to be localized within the cell.

These complexities of G protein signaling in insulation preclude an unambiguous interpretation of genetic-interaction experiments and thus the linking of *moody* to *Gi*/*Go*/*loco* by genetic means. We have generated double-mutant combinations between *moody* and *loco* using genomic mutants as well as RNAi, with indeed complex results: in *moody loco* genomic double mutants, the insulation defect is worse than that of *loco* alone, while in *moody loco* RNAi double mutants the insulation defect is similar to that of *moody* alone (Figure 4C). This strong suppression of *loco* by *moody* is also observed in the survival and motor behavior of the RNAi-treated animals (Figure 4D, Movies S1–S3). Thus, the phenotype of the double-mutant combination is dependent on the remaining levels of *moody* and *loco,* with *moody* suppressing the *loco* phenotype when *loco* elimination is near complete.

Cellular Function of GPCR Signaling in the Surface Glia

To understand how the GPCR signaling components effect insulation at the cellular level, we examined the distribution of different markers in the surface glia under *moody* and *loco* loss-of-function conditions and under glial overexpression of Gi-wt. To rule out cell fating and migration defects, the presence and position of the surface glia were determined using the panglial nuclear marker Repo (Halter et al., 1995). In all three mutant situations, the full complement of surface glia

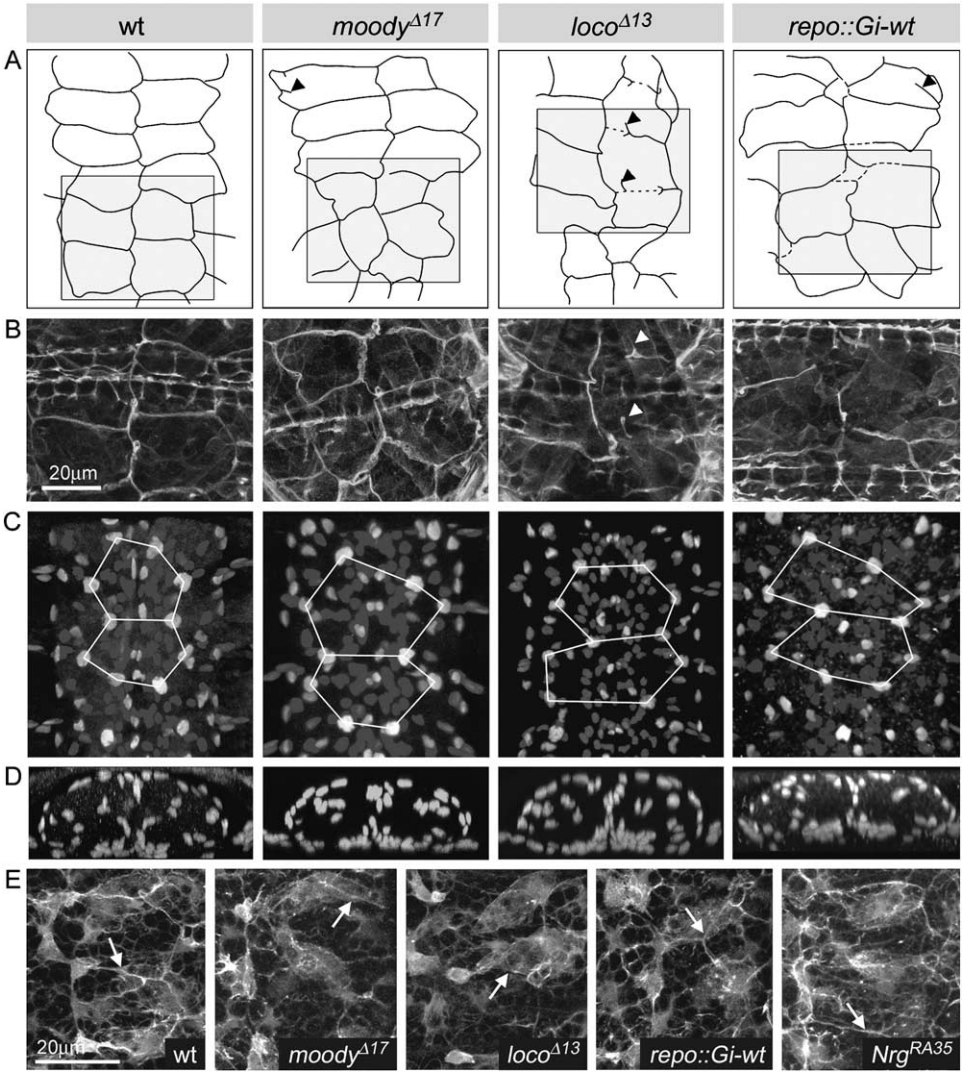

Figure 5. GPCR Signaling Affects Cell Shape, the Accumulation of Cortical Actin, and the Integrity of the Septate-Junction Belt but Not Surface Glial Cell Number or Migration

Images represent projections of confocal stacks: (B) and (E), 10–15 μm total, (C) and (D), 35–45 μm; images show ventral surface views of 18–19 hr embryos, except for (D), which shows transverse views of one segment from confocal stacks in (C).

(A and B) Nrg-GFP expression visualizes the SJ belt and traces surface glial cell outlines; the overlying ectoderm is also labeled, leading to a partial occlusion of the glia. (A) shows tracings of surface glial cell outlines based on confocal images; shaded boxes mark regions shown in higher magnification images in (B). In the three mutant conditions (*moody*$^{\Delta 17}$, *loco*$^{\Delta 13}$, and *repo::Gi-wt*), surface glia show variable cell size and shape. SJ material is unevenly distributed along the junction belt and is occasionally absent (dotted lines in [A]). Nrg-GFP label is frequently found in ectopic locations (arrowheads in [A] and [B]).

(C and D) Repo immunostaining reveals number and position of surface glial nuclei. The normal complement of surface glia is found at the surface of the nerve cord in the different mutants, but the position of the nuclei is more variable than in wild-type, as visualized by overlay of connecting lines. A "blended" projection is used that decreases the brightness of individual sections from ventral to dorsal and thus highlights ventral structures of the nerve cord.

(E) Actin cytoskeleton of the surface glia, as visualized by GFP-Moesin (driven by *repo-Gal4*). In *moody* and *loco* mutants, as well as under Gi-wt overexpression, the cortical actin (arrows) is reduced or absent. By contrast, in the *Nrg* mutant, which lacks SJ, cortical actin appears normal.

is present at the surface of the nerve cord, with the positioning of nuclei slightly more variable than in wt (Figures 5C and 5D).

In the three mutants, the SJ marker Nrg-GFP still localizes to the lateral membrane compartment, but the label is of variable intensity and sometimes absent, indicating that the integrity of the normally continuous circumferential SJ belt is compromised (Figures 5A and 5B). Notably, the size and shape of the surface glia are also very irregular. While qualitatively similar, the phenotypic defects are more severe in *loco* and under Gi-wt overexpression than in *moody*, in line with the results of our functional assays. When examining the three mutants with the actin marker GFP-Moesin, we find that

the cortical actin cytoskeleton is disrupted in varying degrees, ranging from a thinning to complete absence of marker, comparable to the effects observed with Nrg-GFP (Figure 5E). However, GFP-positive fibrous structures are present within the cells, indicating that the abnormalities are largely restricted to the cell cortex. The microtubule organization, as judged by tau-GFP marker expression, appears normal in the mutants (data not shown). The light-microscopic evaluation thus demonstrates that, in the GPCR signaling mutants, the surface glia are positioned correctly and capable of forming a contiguous epithelial sheet as well as septate junctions. Instead, the defects occur at a finer scale—abnormally variable cell shapes and sizes, and irregular distribution of cortical actin and SJ material.

The changes in cell shape and actin distribution that we observe in the three mutants might simply be a secondary consequence of abnormalities in the SJ belt; to test this possibility, we examined how a loss of the SJ affects the morphology and the actin cytoskeleton of the surface glia. SJ components are interdependent for the formation and localization of the septa, and lack of a single component, such as Nrg, leads to nearly complete loss of the junction (Faivre-Sarrailh et al., 2004; Genova and Fehon, 2003) and severe insulation defects (see above). In *Nrg* mutants, the surface glial cell shape and cortical actin distribution show only mild abnormalities (Figure 5E). Thus, in contrast to the GPCR signaling mutants, the complete removal of the SJ causes only weak cytoskeletal defects, strongly arguing against an indirect effect. We conclude that GPCR signaling most likely functions by regulating the cortical actin cytoskeleton of the surface glia, which in turn affects the positioning of SJ material along the lateral membrane.

More detailed insight into the nature of the defects in GPCR signaling mutants is afforded by electron microscopy. We examined the surface glia in nerve cords of first-instar wild-type and mutant larvae. First, dye penetration into the nerve cord was tested using ruthenium red. In wild-type, the dye diffuses only superficially into the surface glial layer, while in *moody* and *loco* mutants the dye penetrates deep into the nerve cord, in concordance with our light-microscopic data (Figures 6F–6I). Tissue organization and SJ morphology were examined under regular fixation in randomly selected transverse sections. Granderath et al. (1999) had reported that the surface glial sheath is discontinuous in *loco* mutant nerve cords, but their analysis was carried out at 16 hr of development, i.e., at a time when, even in wild-type, SJs are not yet established and the nerve cord is not sealed. In contrast to their findings, we observe that, in *loco* as well as *moody* mutants, the glial sheath is in fact contiguous at the end of embryonic development. The ultrastructure of individual septa and their spacing also appear normal, indicating that *moody* and *loco* do not affect septa formation per se. However, the global organization of the junctions within the glial sheath appears perturbed: in wild-type, the surface glia form deep interdigitations (Figure 6B; cf. Carlson et al., 2000), and the SJs are extended, well-organized structures that retain orientation in the same plane over long distances (Figures 6B and 6C). In *moody* and *loco* mutants, the SJs are much less organized; they are significantly shorter in length and do not form long planar extents as in wild-type (Figures 6D, 6E, and 6J).

Taken together, the light- and electron-microscopic evaluations of the GPCR signaling mutants both show defects in the organization of the surface glial epithelium. The reduction in SJ length is consonant with the variability and local disappearance of the Nrg-GFP marker. Since the sealing capacity of the junction is thought to be a function of its length (Abbott, 1991), the reduction in mean SJ length in the mutants provides a compelling explanation for the observed insulation defect.

Discussion

In this study we have examined the formation of the blood-brain barrier in *Drosophila* and its regulation by GPCR signaling. Due to the high potassium content of the hemolymph, flies are very sensitive to a disruption of the barrier. Depending on the severity of the breach, behavioral defects range from mild impairment of motor coordination to complete paralysis. The seal is created by the intercellular SJs formed by the surface glia. The technical difficulty in working with late embryos had hampered the study of the surface glial sheath. By applying live imaging and quantitative measurement of dye penetration, we were able to record its development and begin a genetic dissection of the underlying cellular and molecular processes.

We found that the surface glia coalesce into a single-layer epithelium and form contiguous SJ belts only late in development. As judged by dye occlusion and onset of embryonic movement, the sealing of the nerve cord is complete by 20 hr of development. The orphan GPCR Moody, the G protein α subunits Gi and Go, and their regulator Loco are all (differentially) expressed in the surface glia and, as mutants, show insulation defects, which are manifest in dye penetration and abnormal motor behavior. At the cellular level, the mutants show a variable and often weak distribution of SJ material along the circumference of the glial cells and, ultrastructurally, a shortening of the length of the SJ. Multiple measures thus indicate that GPCR signaling plays a crucial role in the insulation of the nerve cord.

In addition to a reduction of the insulating SJs, our analysis of the GPCR signaling mutants also revealed irregular cell shape and size, as well as weaker and variable accumulation of cortical actin in the surface glia. Our data indeed suggest that the primary defect in the mutants lies with a failure to stabilize the cortical actin, whose proper distribution is required for the complex extended morphology of the glia, which then affects SJ formation as a secondary consequence. Several lines of evidence exclude the reverse chain of causality, that is, a primary SJ defect resulting in destabilization of cortical actin and cell-shape change. Surface glia coalesce into a contiguous sheath and show strong accumulation of cortical actin before SJ material accumulates and sealing is completed. In the GPCR signaling mutants, there is misdistribution of SJ material along the cell perimeter, but the junctions do form. Finally, the GPCR signaling mutants show cell-shape and cortical actin defects that are much more severe than those observed in the near complete absence of SJ.

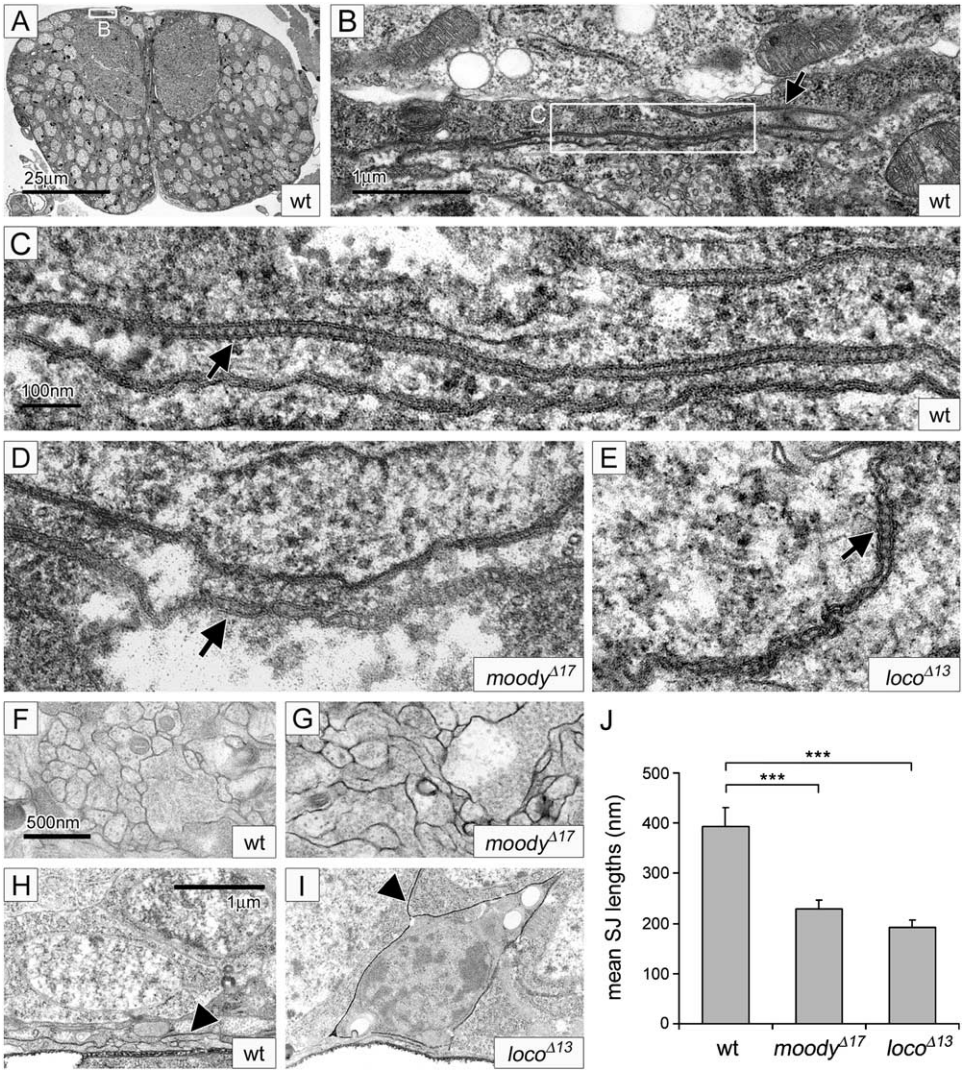

Figure 6. GPCR Signaling Affects Organization and Length of the SJ

(A–E) Conventional electron micrographs of wt (A–C), *moody*$^{\Delta 17}$ mutant hatched (D), and *loco*$^{\Delta 13}$ mutant unhatched (E) 24 hr embryos. White boxes in panels (A) and (B) indicate location of regions shown in higher magnification in (B) and (C). In wild-type, surface glia show deep interdigitations with long SJs (arrows). In the mutants, the surface glia appear less organized and have shorter SJs.

(F–I) Ruthenium-red stainings of wt (F and H), *moody* (G), and *loco* mutant (I) 24 hr embryos. In the mutants but not in wt, the dye penetrates deeply into the nerve cord (arrowheads).

(J) Quantification of SJ length measurements (see Experimental Procedures). Columns represent mean SJ length as measured in random nerve-cord sections, ±SEM, n = 71–75. Brackets indicate statistical significance of comparisons using the t test, ***p < 0.001.

Compared to the columnar epithelia of the ectoderm and the trachea (~5 μm), the surface glial sheath is very thin (~0.5 μm). Compensating for their lack in height, surface glia form deep "tongue-and-groove" interdigitations with their neighbors. This increases the length of the intercellular membrane juxtaposition and thus of the SJ, which ultimately determines the tightness of the seal. We propose that the surface glial interdigitations are the principal target of regulation by GPCR signaling. In GPCR signaling mutants, a loss of cortical actin leads to diminished interdigitation and thus to a shortening of the SJ, resulting in greater permeability of the seal (Figure 7B). This model integrates all our observations at the light- and electron-microscopic levels.

Our proposal that Moody, Gi, Go, and Loco act in a common pathway is principally based on common expression in the surface glia and on the strong phenotypic similarities between these factors at the systemic and cellular level. In addition, we demonstrate physical interaction between Gi, Go, and Loco, thus directly connecting these three components, and show colocalization of the Moody and Loco proteins at the plasma membrane. However, due to the transient nature of receptor-G protein interactions, a physical coupling of Moody with either of the α subunits can only be demonstrated once the ligand is identified. The complexity of this pathway results from the involvement of two different trimeric G proteins that, upon coupling with active receptor, generate three active components (Gi,

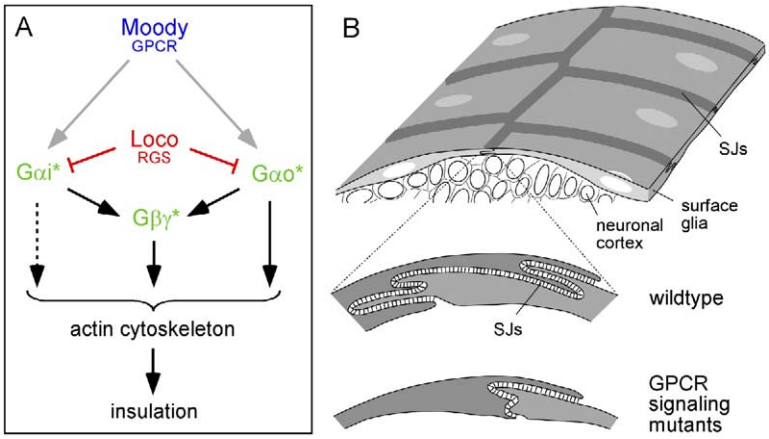

Figure 7. Model of Moody/Loco Signaling and Cellular Function

Schematic depicting the proposed Moody/Loco pathway (A) and its role in regulating surface glial morphology and septate-junction length (B). For description, see text.

Go, and Gβγ) capable of transducing signal to distinct effectors (Neer, 1995). The marked differences in phenotypic strength between the three components strongly support the notion that they do indeed generate distinct outputs in insulation, with activated Go and free Gβγ having a greater role than Gi (Figure 7A). Furthermore, the differences in phenotypic strength between the different agonists (loss of Gβγ > *moody* null > *Gi* null) are inconsistent with a simple linear pathway and suggest that the outputs generated by the G proteins have opposing effects or, quite possibly, that the G proteins receive multiple activating inputs.

A striking feature of Moody/Loco signaling is that both loss of signal (loss of *moody* and *Gi*, quenching of free Gβγ) and gain of signal (loss of *loco*, Go-GTP overexpression) cause qualitatively similar systemic and cellular defects. This phenomenon is characteristic of pathways that generate a localized or graded signal—such a signal will be diminished by loss as well as by uniform excess of activity. The behavior has been observed in contexts such as planar polarity, asymmetric cell division, and axon guidance (Huber et al., 2003; Knoblich, 2001; Mlodzik, 2002). We propose that, in our context, localized G protein activity functions to properly localize or distribute actin at the cell cortex of the surface glia, thereby molding the deep interdigitations critical for insulation. Differential G protein signaling to the actin cytoskeleton has been shown to be responsible for polarized growth in yeast and in *Dictyostelium* and leukocyte chemotaxis (Madden and Snyder, 1998; Manahan et al., 2004; Wu, 2005). Free Gβγ promotes actin polymerization and morphologic extension by localized activation of Cdc42 and Rac, while active Go is likely to promote actin myosin II accumulation and contraction by activation of RhoA. Thus, in these paradigms, the graded distribution of G protein activities sets up a differential localization of two inherently antagonistic processes—expansion and contraction. Our genetic results are consistent with such antagonistic G protein output in insulation. A deeper exploration of the molecular connections between Moody/Loco signaling and the actin cytoskeleton and of the similarities between GPCR signaling in glial ensheathment and in chemotaxis will be a subject of further investigation.

Interestingly, *moody* is required not only for the establishment but also for the maintenance of the blood-brain barrier in adult flies (Bainton et al., 2005), suggesting that the morphology of the surface glia requires continued regulation. Both Moody and Loco are also expressed and required for morphogenesis in other embryonic tissues (T.S. and U.G., unpublished data). Moody's sibling receptor Tre1 has been shown to be necessary for normal germ-cell migration, apparently by signaling through a different pathway (Kunwar et al., 2003). The closest vertebrate homologs of Moody (EX33 and GPR84) are both expressed in migratory blood cells (Wittenberger et al., 2001; Yousefi et al., 2001), and vertebrate homologs of Loco (RGS3 and 4) are upregulated in pathologically motile glioblastoma cells (Tatenhorst et al., 2004). These findings suggest that the GPCR signaling components identified in this study are involved in morphogenetic processes well beyond insects.

Experimental Procedures

Fly Strains and Constructs

The following fly strains were obtained from published sources: *repo-Gal4* (V. Auld); *actin-Gal4* (Y. Hiromi); $nrv2^{G74}$, Nrg^{G305} (Nrg-GFP), and $G\alpha i^{P8}$ (W.Chia); *UAS-GFP-Moesin* (D.Kiehart); *arm-Arm-GFP* (M. Peifer); UAS-tau-GFP (M. Krasnow); Nrx^{4025} (M. Bhat); Nrg^{14} (M. Hortsch); gcm^{N17} (B. Jones); $loco^{\Delta 13}$ (C. Klämbt); *UAS-*$G\alpha i^{wt}$ and *UAS-*$G\alpha i^{GTP}$ (J. Knoblich); and *UAS-*$G\alpha o$, *UAS-*$G\alpha o^{GTP}$, and *UAS-*$G\alpha o^{GDP}$ (A. Tomlinson). *UAS-GFPnuc* was generated by H.Q. Fan (H.Q. Fan and U.G., unpublished data). The $moody^{\Delta 17}$ allele is an imprecise P element excision of *EP1529* and removes the entire ORF of *moody* (=CG4322), CG4313, and part of CG4290 (Bainton et al., 2005). Genomic rescue constructs for the two different *moody* splice forms (*gen-*α and *gen-*β) or both (*gen-*αβ) contain the complete *moody* gene and all intergenic sequences up to the neighboring genes (9.4 kb) (see Bainton et al., 2005). Full-length cDNAs were obtained from the following sources: *moody* (R.J.B.); *tre1* (RT-PCR); and *Gi*, *Go*, *Gs*, *Gq*, and *loco* (DGCr1, BDGP; Stapleton et al., 2002). The frameshift at position 838 of the *loco* cDNA was repaired using a small RT-PCR product.

moody-Gal4 was generated by cloning of the 2.4 kb genomic region directly upstream of the *moody* ORF into the pCasprAUG-Gal4 vector; the construct drives faithful surface-glial-specific expression in third-instar larval nerve cords (Figure S1). *UAS-Loco-GFP* was generated by in-frame fusion of EGFP (pEGFP by Clontech) to the C terminus of the glial-specific variant of Loco (Granderath et al., 1999). *UAS-Moody-mRFP* was generated by in-frame fusion of mRFP (gift from R. Tsien) to the C terminus of the β splice form of Moody; when driven by *repo-Gal4*, the protein fusion rescues $moody^{\Delta 17}$ from 1% to 80% adult viability. *UAS-mRFP-Moesin*

was constructed analogous to the *UAS-GFP-Moesin* reported by Edwards et al. (1997). All constructs were cloned into pUAST (Brand and Perrimon, 1993). UAS marker strains were examined for morphological abnormalities and behavioral/viability problems when expressed in glia (*repo-Gal4*); glial specificity of the *repo-Gal4* driver was established for the late embryo and third-instar larvae (Figure S1). For live genotyping, mutant and transgenic lines were balanced (*Kr::GFP*; Casso et al., 2000) or positively/negatively marked using GFP markers *nrg-Nrg-GFP* and *simu-CD8-RFP* (E. Kurant and U.G., unpublished data). All strains were raised at 25°C.

Immunohistochemistry and Imaging

RNA in situ hybridization was performed as described at http://www.fruitfly.org/about/methods/RNAinsitu.html. Schneider (S2) cells were cotransfected with *actin-Gal4*; *UAS-Loco-GFP*; and *UAS-Gi, Go, Gs,* or *Gq* using cellfectin (Invitrogen) and plated on poly-L-lysine (Sigma) coated coverslips for immunohistochemistry. Immunohistochemistry followed standard procedures using rat anti-Repo (Developmental Studies Hybridoma Bank), anti-GFP (Molecular Probes), rabbit anti-Moody, guinea pig anti-Loco (W. Chia), rabbit anti-Gi (J. Knoblich), rat anti-Go (A. Tomlinson), rabbit anti-RFP (US Biological), fluorescent secondary antibodies (Cy3/Jackson ImmunoResearch; Alexa Fluor 488/Molecular Probes), or Vectastain Elite kit (Vector Labs).

Live imaging was carried out as follows: dechorionated embryos (stage 17) were mounted under halocarbon oil, injected with 100 mM potassium cyanide (2%–3% of egg volume) to subdue their movement, and imaged after 30–60 min incubation. Dissected third-instar larval cephalic complexes were mounted in saline and imaged directly. All confocal images were acquired using a Zeiss LSM 510 system. Stacks of 10–30 0.5 micron confocal sections were generated; image analysis was performed using Zeiss LSM 510 and Imaris 4.0 (Bitplane) software. Colocalization of double-labeled specimens was assessed in 3D using Imaris 4.0. The program calculates colocalization separately for each slice of a confocal stack by computing the geometric mean of the pixel intensities of the two channels after appropriate thresholding. The results for each section are then assembled as a separate channel of the stack. Time-lapse microscopy of 21–22 hr embryos was carried out using a Zeiss Axioplan 2 with MetaMorph software (Universal Imaging Corporation).

For electron microscopy, first-instar wild-type and mutant larvae were processed for conventional EM or ruthenium-red dye penetration by the methods described in Auld et al. (1995). Sections were examined with a Tecnai T12 electron microscope operated at 80 kV, and micrographs were recorded with an AMT or Gatom digital camera. For quantification, random images were shot, and the length of visible SJ membrane stretches in each image was measured using MetaMorph software (Universal Imaging Corporation). Statistics were calculated using the t test.

Embryo Injections and Assays

DsRNA synthesis and microinjection were performed as described by Kennerdell and Carthew (1998). To rule out saturation effects, the total concentration of dsRNA (500–700 bp) was always 5 nmol/ml; for single injections, 2.5 nmol/ml *GFP* dsRNA coinjected with 2.5 nmol/ml with *loco*, *moody*, or *tre1* dsRNA; as control, 5 nmol/ml GFP dsRNA was injected.

For the dye-penetration assay, fluorescent dye (Texas red-coupled dextrane, 10 kDa, 2.5 mM; Molecular Probes) was injected from posterior into the body cavity of 21–22 hr embryos; after 10 min, dye diffusion was analyzed using confocal microscopy. Dye penetration was quantified by calculating the percentage of embryos showing visible dye penetration and as the mean pixel intensity (ranging from 0 to 255) within a representative window of the ventral portion of the nerve cord (n = 31–52). To adjust for variability in laser intensity, autofluorescent *Convallaria* was used for calibration. In addition, background as measured by mean pixel intensity in embryos without dye penetration was subtracted from the mean pixel intensities for all embryos processed in a batch. To assess significance, one-way ANOVA was performed over all groups with Student-Newman-Keuls post hoc test; for the rescue experiments, the χ^2 test was used.

For testing locomotor behavior, the animal's posterior end was gently poked with a needle to trigger an escape response, and body-wall peristalsis/general motility was assessed. The following phenotypic categories were used: (1) hatched larva/normal locomotion, (2) latched larva/peristaltic waves intact/mobility impaired, (3) hatched larva/no peristaltic waves/mobility impaired, and (4) unhatched larva. Eighty-five to one hundred and thirteen animals were analyzed per group, and significance was assessed using the χ^2 test.

Supplemental Data

Supplemental Data include one figures and three movies and can be found with this article online at http://www.cell.com/cgi/content/full/123/1/133/DC1/.

Acknowledgments

We would like to thank V. Auld, M. Bhat, W. Chia, Y. Hiromi, M. Hortsch, B. Jones, D. Kiehart, C. Klämbt, J. Knoblich, M. Krasnow, M. Peifer, A. Tomlinson, R. Tsien, and the Developmental Studies Hybridoma Bank for fly strains, constructs, and antibodies. We are indebted to J. Fak for generating transformants and U. Unnerstall for advice on data analysis and figures. A big thank you goes to Alison North for running a superb Bioimaging Facility and for her magic touch with difficult imaging. This work was supported by NIH grants EY011560 (U.G.), DA14809 (U.H.), and DA444906-33821 (R.J.B.).

Received: October 6, 2004
Revised: May 17, 2005
Accepted: August 22, 2005
Published: October 6, 2005

References

Abbott, N.J. (1991). Permeability and transport of glial blood-brain barriers. Ann. N Y Acad. Sci. *633*, 378–394.

Auld, V.J., Fetter, R.D., Broadie, K., and Goodman, C.S. (1995). Gliotactin, a novel transmembrane protein on peripheral glia, is required to form the blood-nerve barrier in Drosophila. Cell *81*, 757–767.

Bainton, R.J., Tsai, L.T.-Y., Schwabe, T., DeSalvo, M., Gaul, U., and Heberlein, U. (2005). *moody* encodes two GPCRs that regulate cocaine behaviors and blood-brain barrier permeability in *Drosophila*. Cell *123*, this issue, 145–156.

Baumgartner, S., Littleton, J.T., Broadie, K., Bhat, M.A., Harbecke, R., Lengyel, J.A., Chiquet-Ehrismann, R., Prokop, A., and Bellen, H.J. (1996). A Drosophila neurexin is required for septate junction and blood-nerve barrier formation and function. Cell *87*, 1059–1068.

Brand, A.H., and Perrimon, N. (1993). Targeted gene expression as a means of altering cell fates and generating dominant phenotypes. Development *118*, 401–415.

Carlson, S.D., Juang, J.L., Hilgers, S.L., and Garment, M.B. (2000). Blood barriers of the insect. Annu. Rev. Entomol. *45*, 151–174.

Casso, D., Ramirez-Weber, F., and Kornberg, T.B. (2000). GFP-tagged balancer chromosomes for Drosophila melanogaster. Mech. Dev. *91*, 451–454.

Cho, H., Kozasa, T., Takekoshi, K., De Gunzburg, J., and Kehrl, J.H. (2000). RGS14, a GTPase-activating protein for Gialpha, attenuates Gialpha- and G13alpha-mediated signaling pathways. Mol. Pharmacol. *58*, 569–576.

Edwards, J.S., Swales, L.S., and Bate, M. (1993). The differentiation between neuroglia and connective tissue sheath in insect ganglia revisited: the neural lamella and perineurial sheath cells are absent in a mesodermless mutant of Drosophila. J. Comp. Neurol. *333*, 301–308.

Edwards, K.A., Demsky, M., Montague, R.A., Weymouth, N., and Kiehart, D.P. (1997). GFP-moesin illuminates actin cytoskeleton dy-

namics in living tissue and demonstrates cell shape changes during morphogenesis in Drosophila. Dev. Biol. *191*, 103–117.

Faivre-Sarrailh, C., Banerjee, S., Li, J., Hortsch, M., Laval, M., and Bhat, M.A. (2004). Drosophila contactin, a homolog of vertebrate contactin, is required for septate junction organization and paracellular barrier function. Development *131*, 4931–4942.

Freeman, M.R., Delrow, J., Kim, J., Johnson, E., and Doe, C.Q. (2003). Unwrapping glial biology: Gcm target genes regulating glial development, diversification, and function. Neuron *38*, 567–580.

Genova, J.L., and Fehon, R.G. (2003). Neuroglian, Gliotactin, and the Na+/K+ ATPase are essential for septate junction function in Drosophila. J. Cell Biol. *161*, 979–989.

Granderath, S., Stollewerk, A., Greig, S., Goodman, C.S., O'Kane, C.J., and Klambt, C. (1999). loco encodes an RGS protein required for Drosophila glial differentiation. Development *126*, 1781–1791.

Halter, D.A., Urban, J., Rickert, C., Ner, S.S., Ito, K., Travers, A.A., and Technau, G.M. (1995). The homeobox gene repo is required for the differentiation and maintenance of glia function in the embryonic nervous system of Drosophila melanogaster. Development *121*, 317–332.

Huber, A.B., Kolodkin, A.L., Ginty, D.D., and Cloutier, J.F. (2003). Signaling at the growth cone: ligand-receptor complexes and the control of axon growth and guidance. Annu. Rev. Neurosci. *26*, 509–563.

Ito, K., Urban, J., and Technau, G.M. (1995). Distribution, classification, and development of Drosophila glial cells in the late embryonic and early larval ventral nerve chord. Rouxs Arch. Dev. Biol. *204*, 284–307.

Jones, B.W., Fetter, R.D., Tear, G., and Goodman, C.S. (1995). glial cells missing: a genetic switch that controls glial versus neuronal fate. Cell *82*, 1013–1023.

Katanaev, V.L., Ponzielli, R., Semeriva, M., and Tomlinson, A. (2005). Trimeric G protein-dependent frizzled signaling in Drosophila. Cell *120*, 111–122.

Kennerdell, J.R., and Carthew, R.W. (1998). Use of dsRNA-mediated genetic interference to demonstrate that frizzled and frizzled 2 act in the wingless pathway. Cell *95*, 1017–1026.

Knoblich, J.A. (2001). Asymmetric cell division during animal development. Nat. Rev. Mol. Cell Biol. *2*, 11–20.

Kunwar, P.S., Starz-Gaiano, M., Bainton, R.J., Heberlein, U., and Lehmann, R. (2003). Tre1, a G protein-coupled receptor, directs transepithelial migration of Drosophila germ cells. PLoS Biol. *1*, e80. 10.1371/journal.pbio.0000080.

Leiserson, W.M., Harkins, E.W., and Keshishian, H. (2000). Fray, a Drosophila serine/threonine kinase homologous to mammalian PASK, is required for axonal ensheathment. Neuron *28*, 793–806.

Madden, K., and Snyder, M. (1998). Cell polarity and morphogenesis in budding yeast. Annu. Rev. Microbiol. *52*, 687–744.

Manahan, C.L., Iglesias, P.A., Long, Y., and Devreotes, P.N. (2004). Chemoattractant signaling in dictyostelium discoideum. Annu. Rev. Cell Dev. Biol. *20*, 223–253.

McCartney, B.M., McEwen, D.G., Grevengoed, E., Maddox, P., Bejsovec, A., and Peifer, M. (2001). Drosophila APC2 and Armadillo participate in tethering mitotic spindles to cortical actin. Nat. Cell Biol. *3*, 933–938.

Mlodzik, M. (2002). Planar cell polarization: do the same mechanisms regulate Drosophila tissue polarity and vertebrate gastrulation? Trends Genet. *18*, 564–571.

Morin, X., Daneman, R., Zavortink, M., and Chia, W. (2001). A protein trap strategy to detect GFP-tagged proteins expressed from their endogenous loci in Drosophila. Proc. Natl. Acad. Sci. USA *98*, 15050–15055.

Neer, E.J. (1995). Heterotrimeric G proteins: organizers of transmembrane signals. Cell *80*, 249–257.

Parks, S., and Wieschaus, E. (1991). The Drosophila gastrulation gene concertina encodes a G alpha-like protein. Cell *64*, 447–458.

Poliak, S., and Peles, E. (2003). The local differentiation of myelinated axons at nodes of Ranvier. Nat. Rev. Neurosci. *4*, 968–980.

Quan, F., Wolfgang, W.J., and Forte, M. (1993). A Drosophila G-protein alpha subunit, Gf alpha, expressed in a spatially and temporally restricted pattern during Drosophila development. Proc. Natl. Acad. Sci. USA *90*, 4236–4240.

Salzer, J.L. (2002). Nodes of Ranvier come of age. Trends Neurosci. *25*, 2–5.

Schaefer, M., Petronczki, M., Dorner, D., Forte, M., and Knoblich, J.A. (2001). Heterotrimeric G proteins direct two modes of asymmetric cell division in the Drosophila nervous system. Cell *107*, 183–194.

Schier, A.F. (2003). Chemokine signaling: rules of attraction. Curr. Biol. *13*, R192–R194.

Schmidt, H., Rickert, C., Bossing, T., Vef, O., Urban, J., and Technau, G.M. (1997). The embryonic central nervous system lineages of Drosophila melanogaster. II. Neuroblast lineages derived from the dorsal part of the neuroectoderm. Dev. Biol. *189*, 186–204.

Sepp, K.J., and Auld, V.J. (2003). RhoA and Rac1 GTPases mediate the dynamic rearrangement of actin in peripheral glia. Development *130*, 1825–1835.

Snow, B.E., Hall, R.A., Krumins, A.M., Brothers, G.M., Bouchard, D., Brothers, C.A., Chung, S., Mangion, J., Gilman, A.G., Lefkowitz, R.J., and Siderovski, D.P. (1998). GTPase activating specificity of RGS12 and binding specificity of an alternatively spliced PDZ (PSD-95/Dlg/ZO-1) domain. J. Biol. Chem. *273*, 17749–17755.

Stapleton, M., Carlson, J., Brokstein, P., Yu, C., Champe, M., George, R., Guarin, H., Kronmiller, B., Pacleb, J., Park, S., et al. (2002). A Drosophila full-length cDNA resource. Genome Biol. *3*, RESEARCH0080. Published online December 23, 2002. 10.1186/gb-2002-3-12-research0080.

Tatenhorst, L., Senner, V., Puttmann, S., and Paulus, W. (2004). Regulators of G-protein signaling 3 and 4 (RGS3, RGS4) are associated with glioma cell motility. J. Neuropathol. Exp. Neurol. *63*, 210–222.

Tepass, U., Tanentzapf, G., Ward, R., and Fehon, R. (2001). Epithelial cell polarity and cell junctions in Drosophila. Annu. Rev. Genet. *35*, 747–784.

Wittenberger, T., Schaller, H.C., and Hellebrand, S. (2001). An expressed sequence tag (EST) data mining strategy succeeding in the discovery of new G-protein coupled receptors. J. Mol. Biol. *307*, 799–813.

Wolfgang, W.J., Quan, F., Goldsmith, P., Unson, C., Spiegel, A., and Forte, M. (1990). Immunolocalization of G protein alpha-subunits in the Drosophila CNS. J. Neurosci. *10*, 1014–1024.

Wu, D. (2005). Signaling mechanisms for regulation of chemotaxis. Cell Res. *15*, 52–56.

Yarfitz, S., Provost, N.M., and Hurley, J.B. (1988). Cloning of a Drosophila melanogaster guanine nucleotide regulatory protein beta-subunit gene and characterization of its expression during development. Proc. Natl. Acad. Sci. USA *85*, 7134–7138.

Yousefi, S., Cooper, P.R., Potter, S.L., Mueck, B., and Jarai, G. (2001). Cloning and expression analysis of a novel G-protein-coupled receptor selectively expressed on granulocytes. J. Leukoc. Biol. *69*, 1045–1052.

Yu, F., Cai, Y., Kaushik, R., Yang, X., and Chia, W. (2003). Distinct roles of Galphai and Gbeta13F subunits of the heterotrimeric G protein complex in the mediation of Drosophila neuroblast asymmetric divisions. J. Cell Biol. *162*, 623–633.

Yu, F., Wang, H., Qian, H., Kaushik, R., Bownes, M., Yang, X., and Chia, W. (2005). Locomotion defects, together with Pins, regulates heterotrimeric G-protein signaling during Drosophila neuroblast asymmetric divisions. Genes Dev. *19*, 1341–1353.